Performance Report

August 28, 1988 - November 27, 1988

Fifth Quarter(Three Months)

Contract DAAB07-87-C-FO94

With the U.S. Army Night Vision and Electro-Optics Center

Fort Belvoir, Virginia 22060-5677

Contract Monitor: Mr. Fred Carlson

"Two-Photon Absorption Characterization"

Principal Investigators:

Dr. Chris L. Littler

Dr. David G. Seiler

Department of Physics

University of North Texas

Denton Texas, 76203

The views, opinions, and/or findings contained in this report are those of the authors and should not be construed as an official Department of the Army position, policy, or decision, unless designated by other documentation.

Unclassified

SECURITY CLASSIFICATION OF THIS PAGE

REPORT DOCUMENTATION PAGE

Form Approved OMB No 0704 0188

1a. REPORT SECURITY CLASSIFICATION: Unclassified	1b. RESTRICTIVE MARKINGS
2a. SECURITY CLASSIFICATION AUTHORITY	3. DISTRIBUTION/AVAILABILITY OF REPORT: Approved for public release: Distribution is Unlimited
2b. DECLASSIFICATION/DOWNGRADING SCHEDULE	
4. PERFORMING ORGANIZATION REPORT NUMBER(S): NA	5. MONITORING ORGANIZATION REPORT NUMBER(S): NA
6a. NAME OF PERFORMING ORGANIZATION: Univ. of North Texas; 6b. OFFICE SYMBOL (If applicable)	7a. NAME OF MONITORING ORGANIZATION: Center for Night Vision and Electro-Optics
6c. ADDRESS (City, State, and ZIP Code)	7b. ADDRESS (City, State, and ZIP Code): ATTN: AMSEL-RD-NV-IRT Fort Belvoir, VA 22060-5677
8a. NAME OF FUNDING/SPONSORING ORGANIZATION: CNVEO; 8b. OFFICE SYMBOL (If applicable): AMSEL-RD-NV-IT	9. PROCUREMENT INSTRUMENT IDENTIFICATION NUMBER: DAAB07-87-C-F094
8c. ADDRESS (City, State, and ZIP Code): Fort Belvoir, VA 22060-5677	10. SOURCE OF FUNDING NUMBERS: PROGRAM ELEMENT NO. 661102A; PROJECT NO. 1L161110 2A31B; TASK NO. H0; WORK UNIT ACCESSION NO. 007-CJ

11. TITLE (Include Security Classification)

Two Photon Characterization

12. PERSONAL AUTHOR(S)

Chris Littler

13a. TYPE OF REPORT	13b. TIME COVERED	14. DATE OF REPORT (Year, Month, Day)	15. PAGE COUNT
Interim	FROM 8/88 TO 11/88	1/89	17

16. SUPPLEMENTARY NOTATION

17. COSATI CODES			18. SUBJECT TERMS (Continue on reverse if necessary and identify by block number)
FIELD	GROUP	SUB-GROUP	Defect characterization, Magneto-Optical measurements, Two Photon Spectroscopy, Narrow band gap semiconductors II-VI compounds.
17	05		

19. ABSTRACT (Continue on reverse if necessary and identify by block number)

Magneto-Optical measurements of $Hg_{(1-x)}Cd_xTe$ alloys have provided a new means of studying impurities and defects in this important II-VI material. Two-photon magnetoabsorption (TMPA) has been used to accurately determine the temperature dependence of the energy gap of various HgCdTe alloys, revealing behavior that deviates from currently accepted models. In addition, magneto-optical techniques have been used to detect the presence of both shallow and deep impurities/defects and accurately determine their activation energies, thus providing information necessary for understanding the electrical and optical properties of the material.

20. DISTRIBUTION/AVAILABILITY OF ABSTRACT	21. ABSTRACT SECURITY CLASSIFICATION
☐ UNCLASSIFIED/UNLIMITED ☒ SAME AS RPT. ☐ DTIC USERS	Unclassified
22a. NAME OF RESPONSIBLE INDIVIDUAL: Frederick F. Carlson	22b. TELEPHONE (Include Area Code): 703-664-5036; 22c. OFFICE SYMBOL: AMSEL-RD-NV-IT

DD Form 1473, JUN 86 Previous editions are obsolete.

SECURITY CLASSIFICATION OF THIS PAGE

Unclassified

Performance Report
August 28, 1988 - November 27, 1988
Fifth Quarter(Three Months)
Contract DAAB07-87-C-FO94

"Two-Photon Absorption Characterization"

Principal Investigators:
Dr. Chris L. Littler
Dr. David G. Seiler
University of North Texas

According to the Time Phase Task Schedule for the fifth quarter on p. 26 of the proposed technical work, our research investigation and sample characterization has proceeded along the two task categories (b) and (c).

(b) Investigate two-photon absorption...

(c) Identify impurity-related energy levels and correlate...

We shall now address the progress in each of the tasks.

I. (b) Investigate Two-Photon Absorption

The success of the two-photon magnetoabsorption(TPMA) results achieved over the last several months and the need to build up a large data base on TPMA in HgCdTe motivated us to continue TPMA measurements on as many samples of differing x-value as possible. In addition, the temperature dependence of the TPMA structure was obtained for each sample over the widest range of temperature possible in each sample, allowing us to compare our results with that of Hansen, Schmidt, and Casselman(HSC)[1]. This provided a means to test the accuracy of their empirical relationship between the forbidden energy gap and temperature. We now present TPMA results and analysis on four samples of HgCdTe with x-values of 0.235, 0.252, 0.255, 0.276, and 0.298.

n-HgCdTe(x=0.255)

This sample was grown by Texas Instruments using the traveling heater method (THM). It had the following properties:

$$\mu(77K) = 1.19 \times 10^5 \ \frac{cm^2}{V\text{-}sec}$$
$$n(77K) = 2.8 \times 10^{14} \ cm^{-3}$$

Figure 1 shows typical photoconductive spectra for this sample as a function of CO_2 laser wavelength. The two strong resonant peaks corresponding to the TPMA transitions L_1 and L_2 ($a^+(-1) - a^c(1)$ and $b^+(-1) - b^c(1)$, respectively) tabulated in Table 1 of the third quarter report are

clearly seen. Figure 2 shows the comparison between theoretical predictions and the TPMA data, yielding a 7K energy gap (E_g) of 146.5 ± 0.5 meV for this sample. The theoretical lines were calculated using the modified Pidgeon-Brown energy band model and the band parameters listed in last quarter's report.

Figure 2 shows that TPMA provides a very accurate means for measuring the energy gap of HgCdTe, since the two transitions L_1 and L_2 are well described by the theoretical model. As a result, we have studied the temperature dependence of E_g for a variety of samples of differing x-value. An example of the temperature dependence of the TPMA spectra for the THM sample is shown in Figure 3. The magnetic field positions of the TPMA peaks are seen to be relatively independent of temperature from 5K to 15K, and shift to lower magnetic fields at higher temperatures. The temperature-dependent spectra was analyzed using the Pidgeon-Brown model, adjusting only the value of E_g in order to obtain the best fit to the data. The energy gap dependence on temperature is shown in Figure 4, and compared to the predictions of HSC. The energy gap is seen to be relatively independent of temperature between 5K and 15K and increases with a slope that is somewhat different than that predicted by the HSC relation. In addition the "flattening" of the energy gap observed at temperatures below 15K is not predicted by the HSC relationship. This "flattening" is, however, commonly observed in other semiconductors[2].

Figure 5 shows the temperature dependence of E_g for 4 samples of HgCdTe of differing x-value. In each case, the HSC prediction (solid line) was obtained by matching the highest temperature data point(s) to the HSC prediction, since the HSC predictions appear to better match the experimental data at higher temperatures. The x-value listed in the figure is thus the result of this fit. We see that the deviation between the measured energy gap vs temperature and that of the HSC model predictions becomes larger with larger x-value. As a result we developed a new empirical expression that better describes the temperature dependence of the energy gap of HgCdTe. The results are shown in Figure 6 for the same 4 samples shown in Figure 5. The expression used to describe the data shown in Figure 6 was obtained by incorporating a Varshni-like[3] expression, commonly used to describe the temperature dependence of E_g in other semiconductors, into the HSC relationship. The resulting expression is

$$E_g(x,T) = -.302 + 1.93x + \left(\frac{\alpha T^3}{\beta + T^2}\right)(1-2x) - 0.81x^2 + 0.832x^3 \qquad (1)$$

where α and β are constants which are different for different x-values. We see from Figure 6 that Equation 1 describes well the temperature dependence of all samples measured to date. We are currently working on the development of universal expressions for α and β that correctly describe the temperature dependence of all HgCdTe alloys.

II. c. Identify impurity-related levels and correlate...

In addition to one-photon interband, two-photon interband, and impurity-to-band magnetoabsorption processes which we have reported on so far, most magneto-optical spectra also contains wavelength-independent structure. Figure 7 shows one of the first observations of this structure. This resonant structure has been seen only in the photoconductive response and is also observed only for high laser intensities and in the presence of interband absorption. In the first year an initial attempt was made to explain the data and the following models were considered:

(1) Shubnikov-de-Haas oscillations resulting from an accumulation layer at the surface of the sample.

(2) Impurity-assisted magnetophonon oscillations.

(3) Magneto-impurity oscillations.

After detailed consideration of these models (discussed in the interim annual report) it was determined that only impurity-assisted or magneto-impurity oscillations could be responsible for the observed oscillations. During the fifth quarter it was also determined that these oscillations were seen only when magneto-optical transitions from the shallow acceptor level to the conduction band were observed. Figure 8 shows clearly all three processes: (1) the large peak is due to one-photon interband magnetoabsorption, (2) the weaker resonance is due to impurity-to-band magnetoabsorption involving a shallow acceptor impurity, and (3) the small oscillatory structure shown at lower magnetic fields is the wavelength-independent oscillations under discussion.

In order to better interpret the wavelength-independent structure, magnetic field modulation techniques were employed to increase the resolution of the oscillations. An example of the improved resolution is seen in Figure 9. A total of 10 resonances are clearly resolved. To explain this data, we adopted the magneto-impurity effect model, which involves resonant scattering of carriers between impurity levels and Landau levels such that oscillations are observed whenever[4]

$$n\hbar\omega_C = E_2 - E_1 \quad ,$$

where E_2 and E_1 are the energies of two impurity states, one of which is usually the ground state, and $\hbar\omega_C$ is the energy separation between Landau levels. Since the impurity that dominates the magnetoabsorption spectra is the shallow acceptor level, the MI oscillations involve resonant scattering between the heavy-hole Landau levels and this shallow acceptor's ground and excited states. Figure 10 shows the result of fitting the data presented in Figure 9 using the MI model. The solid lines represent the energy separation between the lowest lying heavy-hole Landau levels (both + and - spins) and successive heavy hole levels, or, equivalently, the field dependence of $n\hbar\omega_C$, and the solid boxes are the magnetic field positions of the MI resonances. A good fit is clearly obtained when $E_2 - E_1 = -4.25$ meV. This energy corresponds closely to that expected for the energy separation between the first excited state of the shallow acceptor to the valence band continuum.

In order to verify the involvement to the shallow impurity in the observed resonant structure, a temperature dependence of the oscillations was recorded. A example of this is shown in Figure 11. The strength of the oscillations are seen to be strongly temperature dependent, essentially vanishing above 21 K. This would be expected if the energy states of a shallow impurity played a role in the oscillations, since they are rapidly ionized with increasing temperature. The resonant structure also moves to higher magnetic field with increasing temperature, consistent with the model.

References:

1. G. L. Hansen, J. L. Schmidt, and T. N. Casselman, J. Appl. Phys. 53, 7099 (1982).
2. C. L. Littler and D. G. Seiler, Appl. Phys. Lett. 46, 986 (1985).
3. Y. P. Varshni, Physica 34, 149 (1967).
4. L. Eaves and J. C. Portal, J. Phys. C: Solid State Physics 12, 2809 (1979).

Figure 1. Wavelength dependence of photoconductive spectra for the TI THM sample.

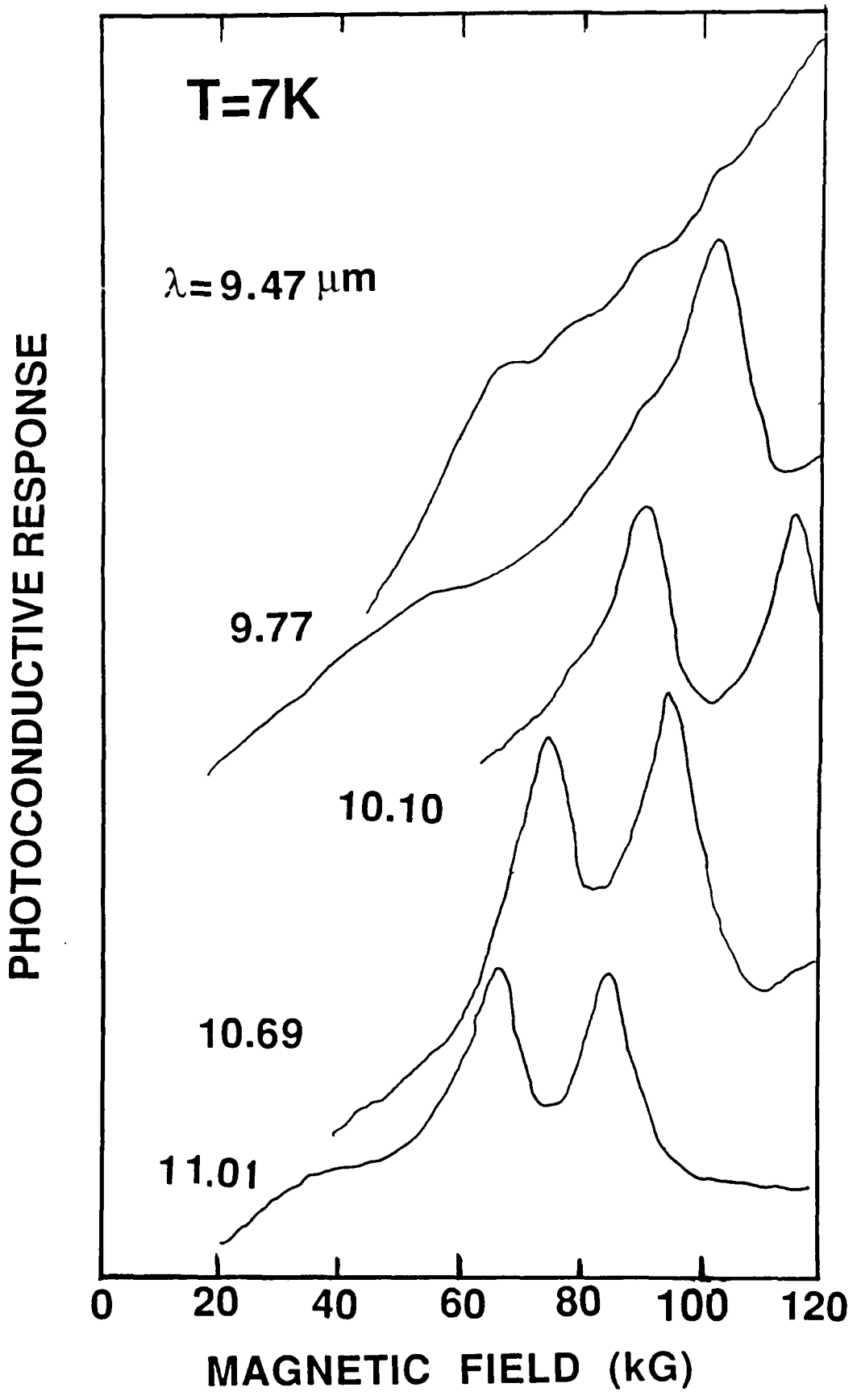

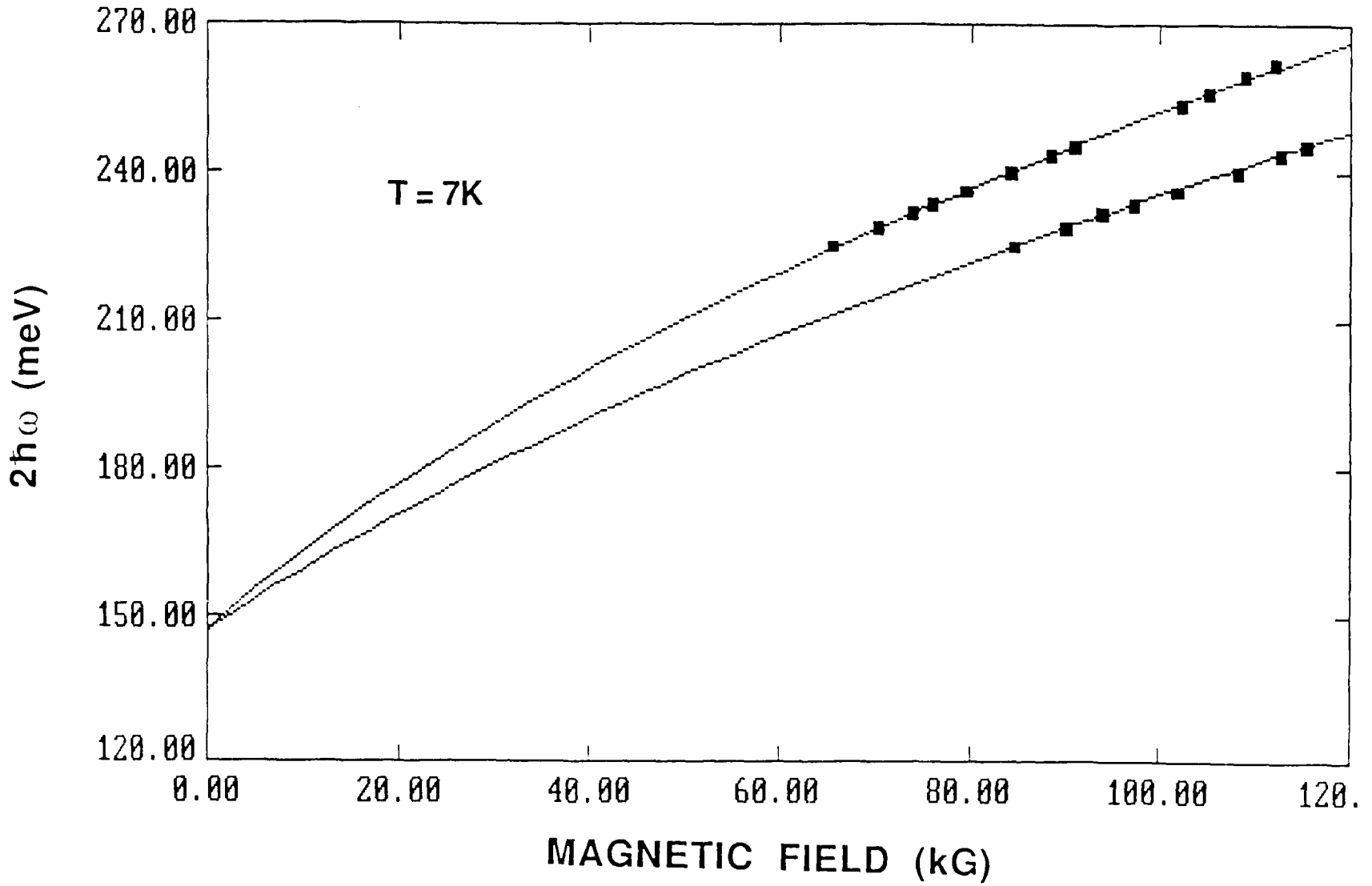

Figure 2 Transition energy vs. magnetic field for the TPMA spectra from the TI thm sample. The 7K energy gap from the fit of theory (solid lines) to data(solid boxes) is 146.5 meV.

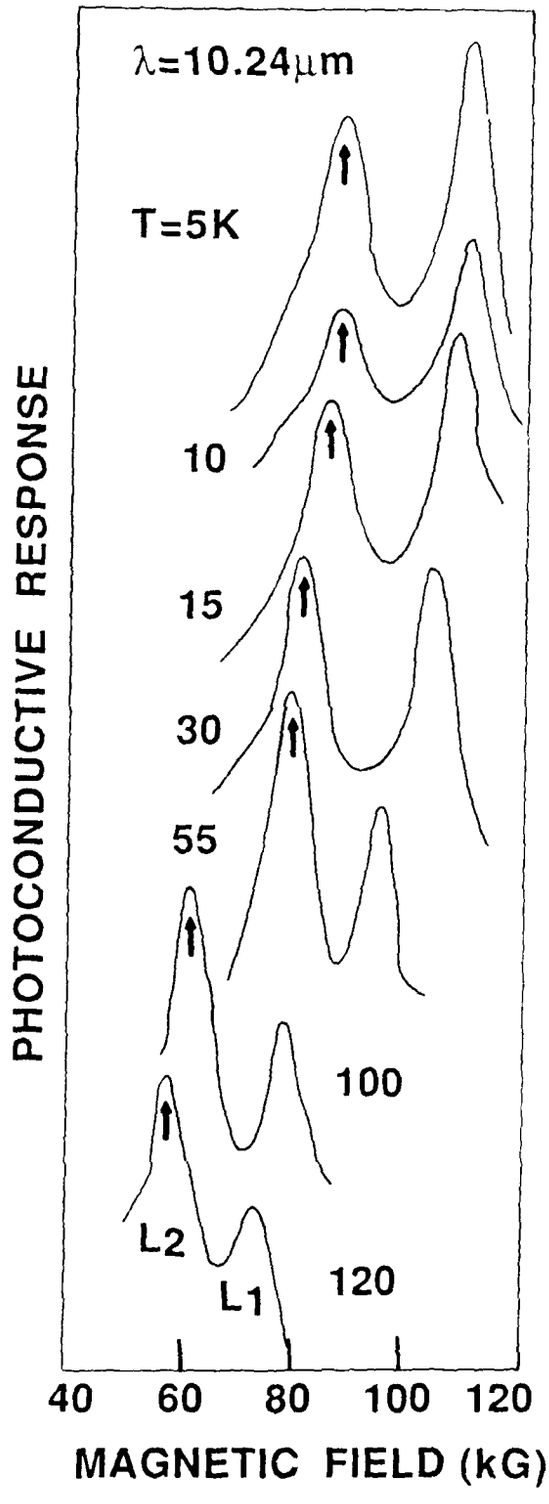

Figure 3. Temperature dependence of the photoconductive spectra for the TI THM sample.

Figure 4. Energy gap dependence on temperature for the TI THM sample. Solid line shows the HSC prediction of this x-value sample.

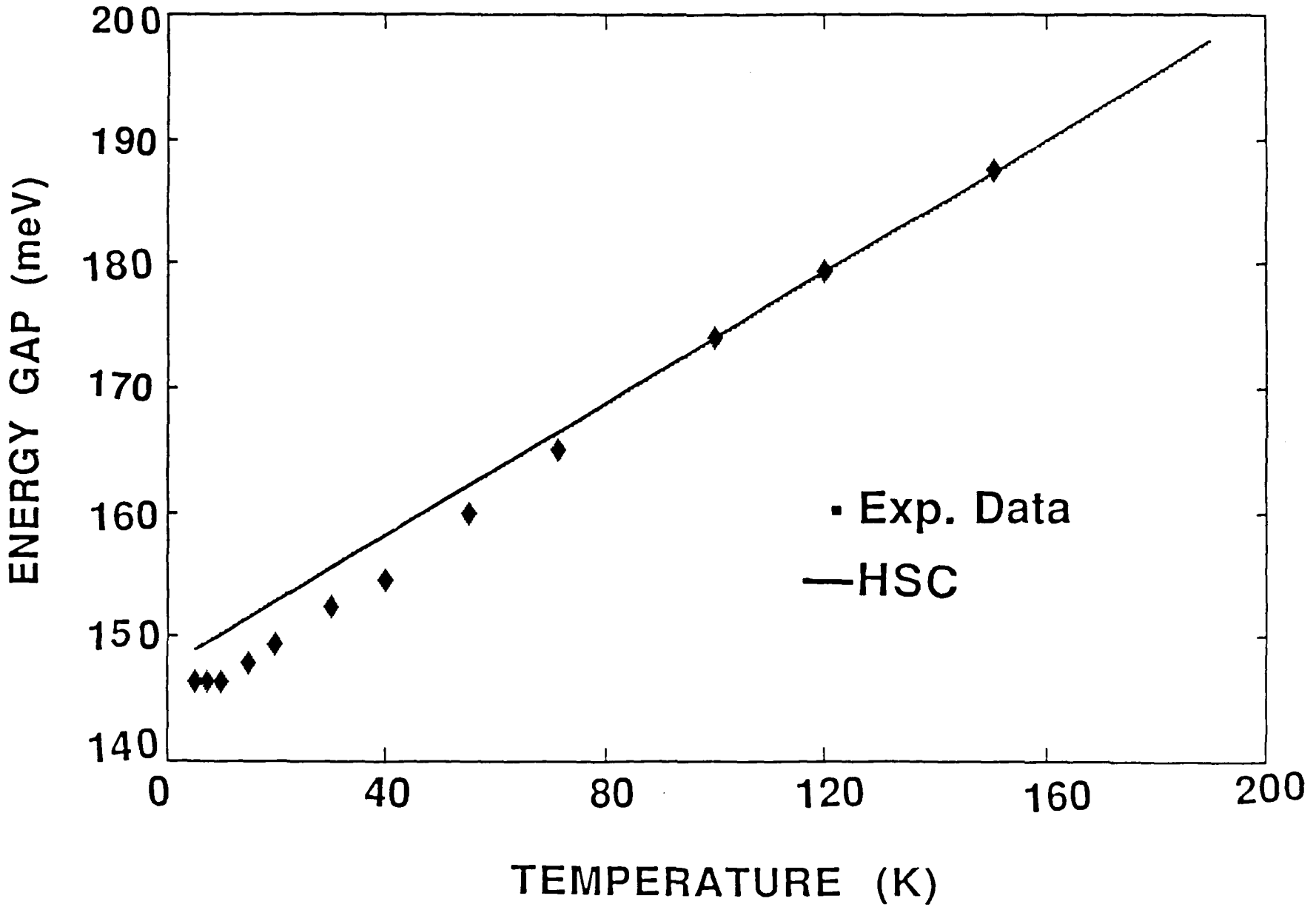

Figure 5. Energy gap dependence on temperature for 4 samples, ranging in x-value from 0.240 to 0.305. The x-values listed are obtained from fit of the HSC relation to the high temperature data.

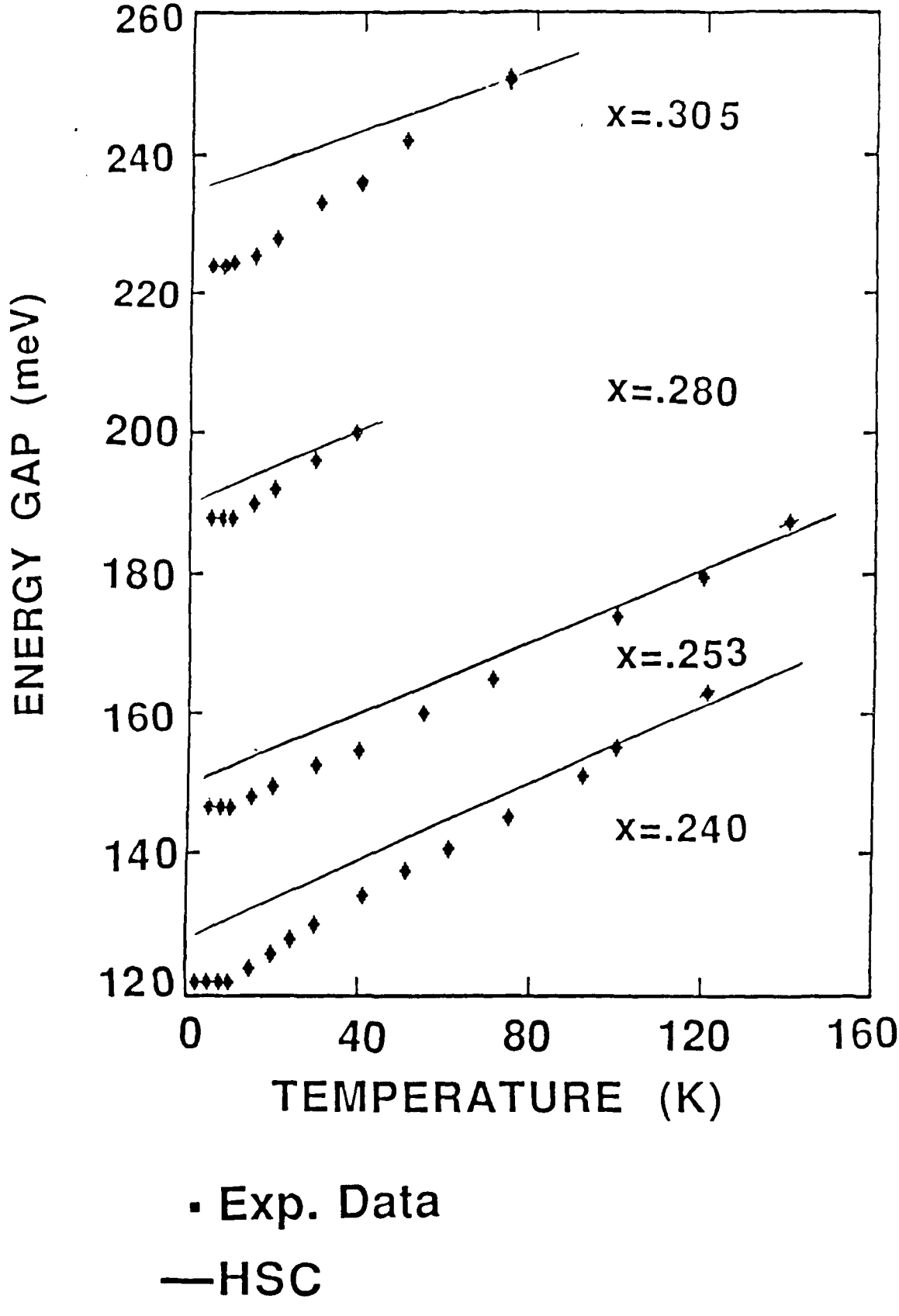

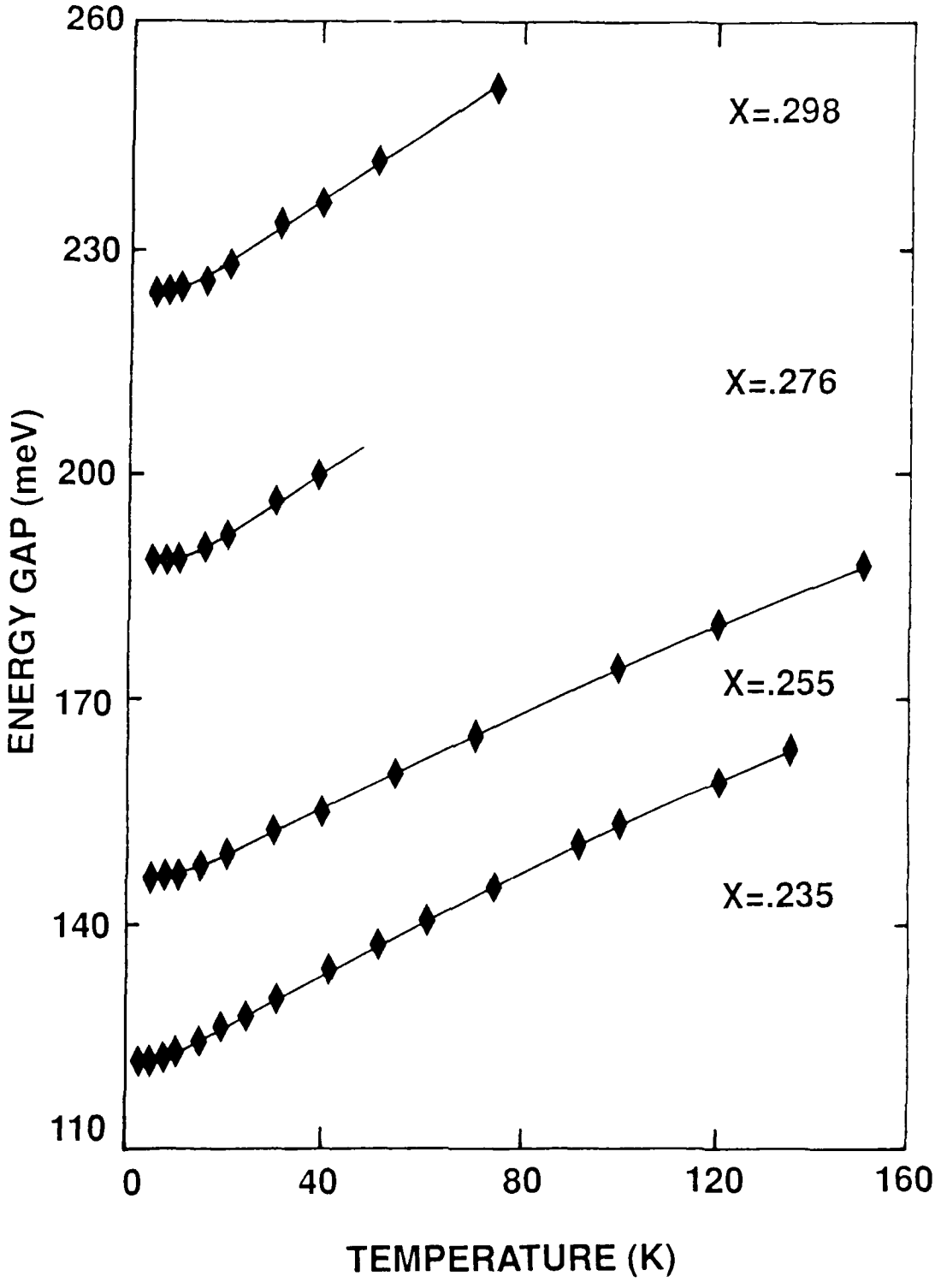

Figure 6. Energy gap dependence on temperature for 4 samples of HgCdTe. The fit was obtained using our new empirical expression.

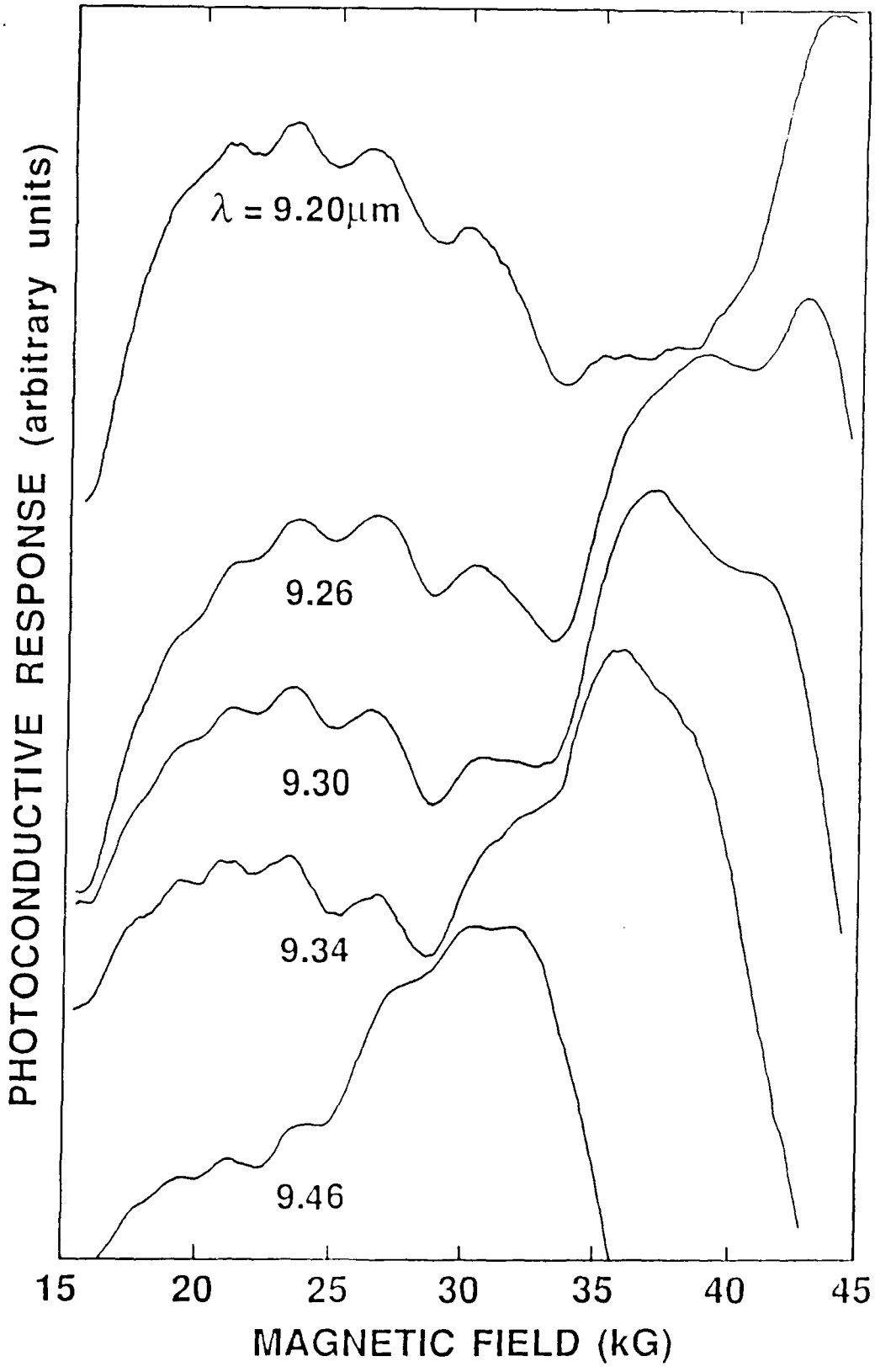

Figure 7 Wavelength dependence of the high intensity structure showing the movement of the one-photon magneto absorption (OPMA) structure against the high intensity structure.

Figure 8. Photoconductive response versus magnetic field for an x = 0.237 sample of HgCdTe. The spectra shows three features: (1) one-photon magnetoabsorption(large peak),(2) impurity magnetoabsorption(small peak), and (3) magneto-impurity (MI) oscillations (small, oscillatory structure).

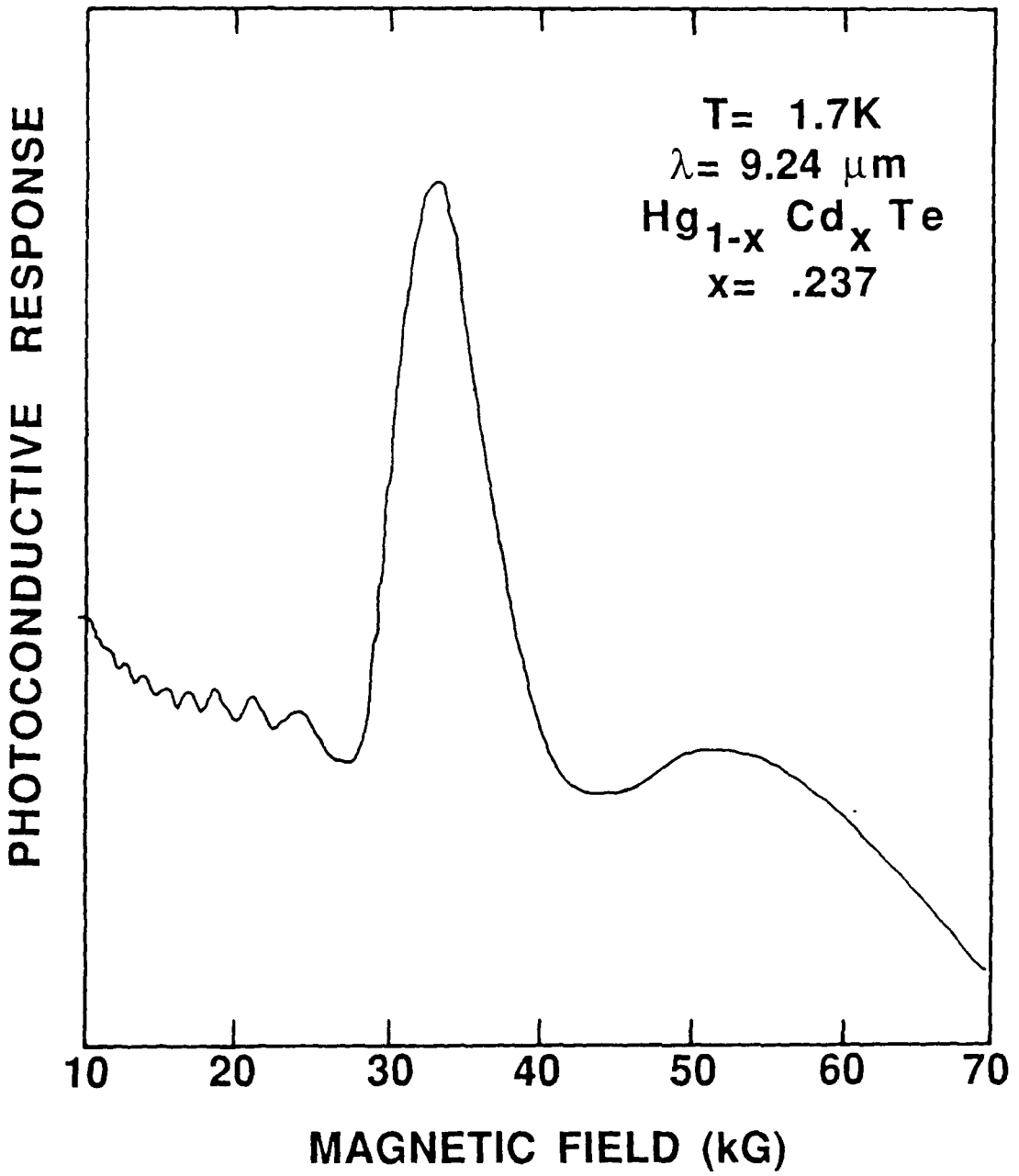

Figure 9. High resolution MI spectra. The data was obtained using magnetic field modulation techniques and represents the 2nd derivative of the photoconductive response vs magnetic field.

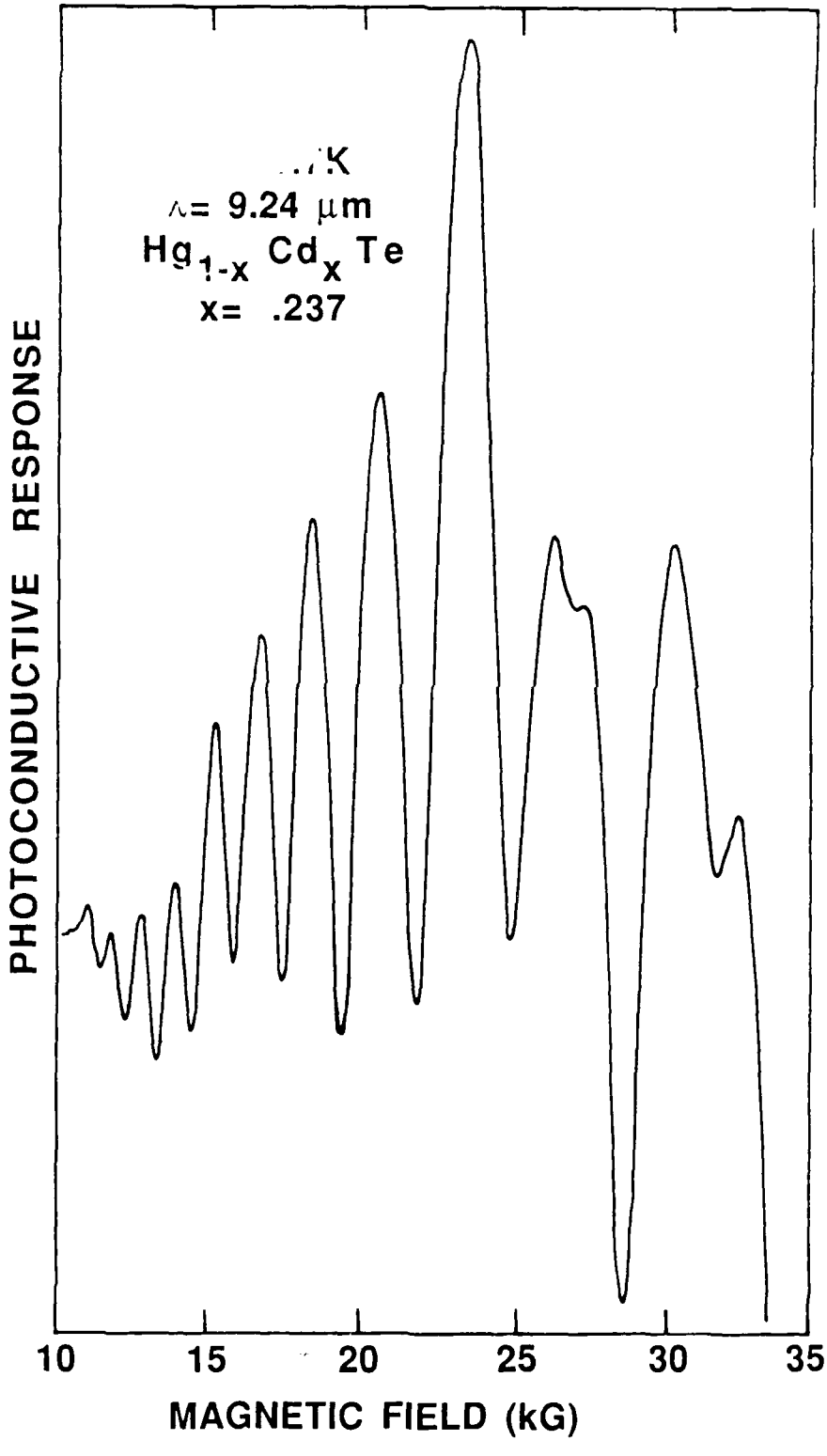

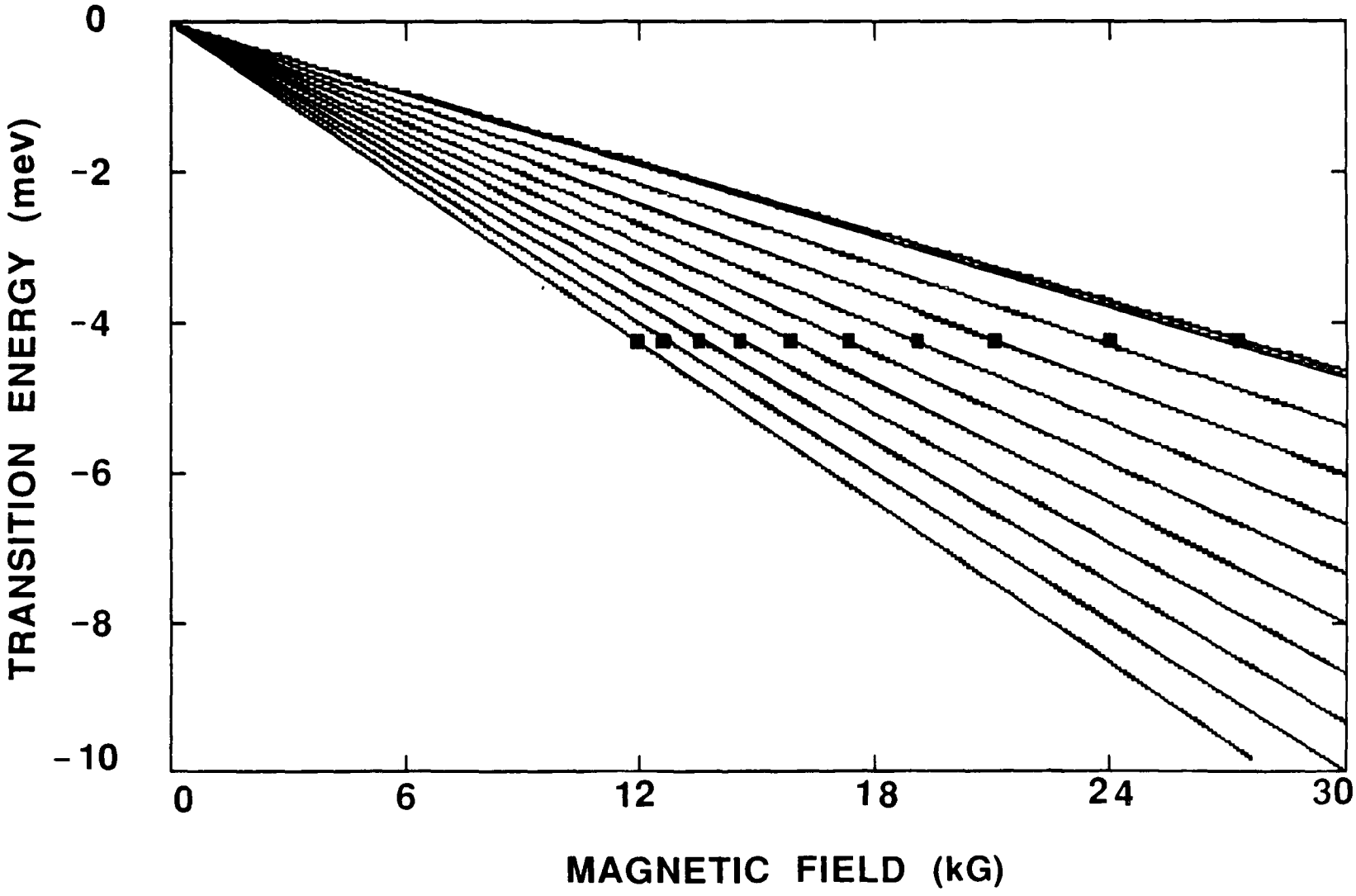

Figure 10. Analysis of MI data. Solid lines represent $n\hbar\omega_c$ energies and open boxes represent the data.

Figure 11. Temperature dependence of the magneto-impurity oscillations.